Polymer Bulletin 20, 75–82 (1988)

Polymer Bulletin

Intramolecular dynamics of polystyrene in good solvents

A.M. Jamieson

Case Western Reserve University, Department of Polymer Science, Institute of Technology, Cleveland, OH 44106, USA

ABSTRACT

Dynamic light scattering data are interpreted to obtain the longest intramolecular relaxation time, τ_1 and the relative amplitude of the scattering from intramolecular and center of mass translational diffusive decay modes, P_o/P, for a polystyrene (PS) of high molecular weight $M_w = 8.42X10^6$, in two good solvent systems, ethylbenzene (ETBZ) and tetrahydrofuran (THF) at 25°C. Comparison of τ_1 data with the Rouse-Zimm theory, $\tau_1=M[\eta]\eta_s/A_1RT$, indicates differences in the value of the draining parameter A_1 between these two solvent systems. In addition, the relative scattering amplitude of the diffusive scattering for a single coil, $(P_o/P)_{c=o}$, decreases more rapidly with qR_g for PS in THF. Thus the scattering amplitude of the intramolecular normal modes of motion of PS in THF, for a specified value of qR_g are substantially larger than those for PS in ETBZ and the other aromatic good solvents. These observations are each qualitatively consistent with a larger solvent draining effect in ETBZ versus THF. Comparison with literature data for chains in good and theta solvents suggests that the quantity $(P_o/P)_{c=o}$ may be a universal function of qR_h.

INTRODUCTION

Experimental data on the transport properties of polymer chains in dilute solutions suggest the existence of non-universal characteristics in the hydrodynamic interactions[1-5]. Possible mechanisms for these effects are variations in the degree of solvent draining[5,15], internal friction[12] or chain rigidity[8]. Our own recent work has focused on a comparative study of polystyrene in the two chemically dissimilar good solvents, tetrahydrofuran and ethylbenzene. Significant numerical differences were found in the ratios $\rho_1=R_g/R_{h,f}$ and $\rho_2=R_{h,\eta}/R_{h,f}$, where R_g is the radius of gyration and $R_{h,f}$ and $R_{h,\eta}$ are the hydrodynamic radii determined from the frictional coefficient and intrinsic viscosity, respectively[4,9]. Measurements of the mean decay rate, Γ_e, of the dynamic light scattering structure factor, in the intermediate scattering vector regime, $qR_g \gtrsim 1$, also showed differences between PS/THF and PS/ETBZ, provided the reduced quantity $\Gamma^* = \Gamma_e(c=o)/q^3kT/\eta_o$ were compared[9]. These results were interpreted to indicate differences in chain hydrodynamics for the two solvents, viz. the presence of a larger solvent draining effect for PS/ETBZ. Similar non-universal effects have been observed in ρ_1, ρ_2 and Γ^* for other polymer solvent systems[6-8,10]. At present there is no consensus as to the theoretical modeling of these properties[5,11-15].

In dynamic light scattering experiments at intermediate q vectors it is possible, in principle, to separately evaluate the contributions from center of mass translational diffusion and intramolecular dynamics. Such analyses involve difficult questions regarding the uniqueness of the spec-

tral decomposition and have been described in only a few cases[6-8]. Information on the relaxation time for the slowest intramolecular normal mode τ_1 and the relative scattering amplitude of the diffusive component $(P_o/P)_{c=o}$ for a single coil can be obtained. Theoretical predictions for τ_1 and $(P_o/P)_{c=o}$ have been reported for gaussian coils[17,19] near the non-draining Zimm limit. Experimental data for linear flexible chains at the theta condition appear to be consistent with this theory[17,19]. On the other hand, while τ_1 values for chains in good solvents[7,8] are reported to be in agreement with the non-draining limit, the $(P_o/P)_{c=o}$ data show substantial deviations from the gaussian chain prediction[19] in a direction qualitatively consistent with an increase in solvent draining on chain expansion.

In this communication we summarize results of dynamic light scattering (DLS) measurements over a wide range of scattering wave vectors extending to $qR_g \cong 4.0$ for a high molecular weight atactic polystyrene ($M_w=8.42X10^6$) in ETBZ and in THF. The DLS relaxation spectrum has been successfully resolved into a slow mode corresponding to pure translational diffusion and a fast mode containing information on intramolecular motion. The parameters determined are the longest intramolecular relaxation time, τ_1, and the relative scattering amplitude of the translational diffusive mode, P_o/P, at infinite dilution. These are contrasted for PS in ETBZ and in THF and are further compared with literature data for linear chains in good and theta solvents.

Our results indicate that the scattering amplitude of the normal mode type configurational motions of polystyrene in tetrahydrofuran for a specified value of qR_g are comparable to those observed in the theta solvents and are substantially larger than those in ethylbenzene and the other aromatic good solvent systems, benzene and toluene. The parameter qR_h appears to be a more universal scaling parameter for the partitioning of the total scattering amplitude between internal and external relaxation mechanisms. Comparison of τ_1 data normalized for solvent viscosity indicates substantial differences in the molecular hydrodynamic behavior of PS/THF versus PS/ETBZ. These experimental results are clearly of interest in view of the fact that current theoretical models of single coil hydrodynamics have not as yet led to conclusive results[12].

All dynamic light scattering experiments were performed on a Brookhaven Instrument Corp. spectrometer comprising a BI 2000 goniometer and a BI 2030AT correlator with a SpectraPhysics 15 mW He/Ne laser (λ = 6328A). The intensity autocorrelation function, $G^2(\tau)$ was measured on a BI 2030AT 264 channel multiple sampling time correlator described elsewhere[9]. Groups of 64 channels could be set to different sample times enabling us to probe relaxation processes occurring on widely differing time scales simultaneously. Hence, we could accurately resolve the spectrum into contributions from pure translational diffusion and intramolecular motion.

Polystyrene samples of weight average molecular weight, $M_w=8.42X10^6$, and M_w/M_n = 1.17 were obtained from Pressure Chemicals (Pittsburgh) and were used without further purification. These samples were characterized by methods of static light scattering in our laboratory. The solvents, spectrograde tetrahydrofuran and ethylbenzene, were obtained from Aldrich Chemical Co. The solvent ETBZ was used without further purification while, due to its hygroscopic nature[29], THF was further purified by refluxing with $LiAlH_4$ for 12 hours and then distilling in a dry inert N_2 atmosphere immediately before use. The refractive index of the solvents at 25°C was determined to be $(THF)n_{25^oC}$ = 1.407 and $(ETBZ)n_{25^oC}$ = 1.495. The specific refractive index increment, dn/dc, of PS in THF and ETBZ at 6328A was measured to be dn/dc=0.192 cc/g and dn/dc=0.111 cc/g at 25°C respectively. The viscosity of the solvents was measured at 25°C using a Cannon Ubbelohde Viscometer and was determined to be 0.465 cp (THF) and 0.619 cp (ETBZ).

Dilute solutions of PS in THF and ETBZ were made by weighing individual samples in a Perkin Elmer microbalance, Model AD-2 with an accuracy of ± .01 mg. The method of solution preparation has been described in detail elsewhere[9]. All measurements were made from 20 to 120 degrees scattering angle. Only those intensity-intensity time correlation functions $G^2(\tau)$, where the difference between the calculated and measured baselines was less than 0.1% were used for data analysis. The data were further analyzed on an IBM/AT computer and a VAX 11/780 as described below.

The static parameters, M_w and $R_{g,z}$, were determined from square-root plots[20] of $[Kc/\Delta R(\theta)]^{\frac{1}{2}}$ versus $\sin^2\theta/2+kc$, where K is an optical constant, $\Delta R(\theta)$ is the excess Rayleigh Ratio , θ is the scattering angle and c is the polymer concentration in g/ml. The dynamic quantities determined were the z-average translational diffusion coefficient $D_{t,z}$, the corresponding Stokes Radius, R_h, the collective intramolecular relaxation, τ_c, and the relative amplitude of the translational diffusive motion, P_o/P. The average decay rate, Γ_e, in the angular range $qR_g<1.0$ was determined by cumulant[21] analysis of the correlation function. Here the scattered electric field autocorrelation function can be expressed as

$$\ln g^1(\tau) = -\Gamma_e\tau + \mu_2\tau^2/2\mu_e^2 - \mu_3\tau^3/6\Gamma_e^3 + \ldots \quad (1)$$

and

$$g^1(\tau) = \int_0^\infty G(\Gamma)\exp(-\Gamma\tau)d\Gamma \quad (2)$$

is related to the measured intensity-intensity correlation function $G^2(\tau)$ by Siegert[22] relation. From the average decay rate Γ_e

$$\Gamma_e = \int_0^\infty G(\Gamma)\Gamma d\Gamma \quad (3)$$

we obtain the z-average translational diffusion coefficient $\langle D_t\rangle_z$ since

$$\Gamma_e = \langle D_t\rangle_z q^2 \quad (4)$$

where $q = 4\pi n_o \sin\theta/2/\lambda$ is the scattering vector.

However, as the scattering vector increases, the experimental parameters extend into the intermediate qR_g region, $qR_g>1$, where the decay rate distribution function $G(\Gamma)$ contains information about the translational diffusion as well as configurational or internal motions[22]. Here, the correlation function becomes increasingly nonexponential due to contributions from intramolecular motions and multi-modal distributions are obtained. This is evident in the presence of a second relaxation process, Γ_2,

$$\Gamma_2 = Dq^2 + 2/\tau_1 \quad (5)$$

where τ_1 is the relaxation rate of the first normal mode of motion. As the scattering wave vector, qR_g, increases further, the fraction of the total scattered intensity arising from pure translational diffusion further decreases. This is due to the fact that the contribution from intramolecular motions increases due to the presence of additional relaxation modes[19,22].

$$\tau_{2N} = Dq^2 + 2/\tau_N \quad (6)$$

where the internal modes of the N^{th} order have a relaxation time τ_N.

For our experiments in the intermediate qR_g region, two approaches have been applied to separate the internal and external scattering components in conjunction, viz. the double-exponential (DEXP) and the Multi-exponential

(MEXP) fitting techniques. The Multi-exponential sampling technique[26-28] approximates $G(\Gamma)$ by a set of logarithmically spaced discrete single exponentials

$$G(\Gamma) = \sum_j P_j \delta(\Gamma - \Gamma_j) \tag{7}$$

where P_j are the weighting factors of the δ function and

$$\sum_j P_j = 1 \quad \text{(normalization condition)}$$
$$\Gamma_j/\Gamma_{j-1} = K \quad (K = \text{constant}).$$

Substituting for $G(\Gamma)$ in equation (2) yields

$$|g^1(\tau)| = \sum_j P_j \exp(-\Gamma_j \tau) \tag{8}$$

where each of the P_j contributions is linearly independent. Then a linear least squares procedure is used where

$$\sum_{i=1}^{M} [G^2(\tau) - \sum_{n=1}^{N} a_n \exp(-\Gamma_i \tau)]^2 \tag{9}$$

is minimized and a semi-log plot of a_n vs Γ is obtained. The values of the average decay rate, Γ_e, are obtained reproducibly, with high precision from the $G(\Gamma)$ function determined from this analytical technique. On the other hand, the precise form of the $G(\Gamma)$ function may or may not be an accurate description of the true bimodal function implicit in the relaxation spectrum,[23].

The DEXP method approximates the $G(\Gamma)$ distribution as a weighted sum of two Dirac delta functions,

$$G(\Gamma) = a_1 \delta(\Gamma - \Gamma_1) + a_2 \delta(\Gamma - \Gamma_2) \tag{10}$$

which corresponds to

$$|g^1(\tau)| = [a_1 \exp(-\Gamma_1 \tau) + a_2 \exp(-\Gamma_2 \tau)] \tag{11}$$

where a_1 and a_2 are the amplitudes of the scattered intensity corresponding to the characteristic linewidths Γ_1 and Γ_2. Therefore, $a_1 + a_2 = 1$ and $\Gamma_e = a_1\Gamma_1 + a_2\Gamma_2$. At scattering wavevectors, $qR_g > 1.0$, the $G(\Gamma)$ distribution can be efficiently extracted using the DEXP analyses mentioned above. The slow mode, Γ_1 is assigned[22] to pure translational diffusion,

$$\Gamma_1 = Dq^2 \tag{12}$$

and the infinite dilution translational diffusion coefficient is obtained by extrapolation from

$$\langle D_t \rangle_z = \langle D_t^o \rangle (1 + k_D c) \tag{13}$$

The concentration dependence of $\langle D_t \rangle_z$ is evaluated by

$$K_d = 1/\langle D_t^o \rangle_z \cdot (d\langle D_t \rangle_z / dc)_T \tag{14}$$

and the average hydrodynamic radius $\overline{R}_h$ ($= \langle R_h^{-1} \rangle_z^{-1}$) is obtained from the Stokes-Einstein equation,

$$\langle D_t \rangle_z = kT/6\pi\eta_o R_h \tag{15}$$

where η_o is the measured viscosity.

Similarly, the second mode Γ_2 may be expressed as

$$\Gamma_2 = Dq^2 + 2/\tau_c \tag{16}$$

where τ_c is a collective intramolecular relaxation time measured at a finite scattering angle. In the limit of infinite dilution and zero scattering angle, τ_c yields the longest intramolecular time τ_1,

$$\lim_{c,q\to o} \overline{\Gamma}_2 - \overline{\Gamma}_1 = 2/\tau_1 \tag{17}$$

Since Γ_e values are determined reproducibly with high accuracy by the MEXP analysis, we followed a procedure in which the Γ_e values were first determined by MEXP, and subsequently bimodal fits to eq. (11) were made using the DEXP program which employs an equally weighted nonlinear regression procedure according to Marquardt[24]. In our DEXP fits, the values of the average linewidth, Γ_e, were constrained to those obtained from the MEXP analysis. A number of simulated experiments were performed and the reliability of this calculation procedure was confirmed.

RESULTS

All our data were processed to determine Γ_1 and Γ_2 for the slow and fast modes. After extrapolation to c=o we obtained $\overline{\Gamma}_1(c=o)$ and $\overline{\Gamma}_2(c=o)$. In Figure 1 we show the angular dependence of $\overline{\Gamma}_1/q^2$ and $\overline{\Gamma}_2-\overline{\Gamma}_1$, respectively. From this plot we determined $D^o_{t,z}=\overline{\Gamma}_1/q^2$ and $2/\tau_c=\overline{\Gamma}_2-\overline{\Gamma}_1$. The results of our static and dynamic measurements for PS in THF and ETBZ at 25°C are summarized in Table 1. We have determined the z-average translational diffusion coefficients, $D^o_{t,z}$, their concentration dependence, K_d, the equivalent hydrodynamic radii, R_h, and the longest intramolecular relaxation time, τ_1. Also listed are the radii of gyration, $\langle R_g\rangle_z$, the second virial coefficients, A_2, ratios of the static to dynamic radii, $\rho=R_{g,z}/\langle R_h^{-1}\rangle^{-1}$ and values of the interpenetration parameter, ψ.

We have deduced from our earlier experiments[4,9] that ETBZ and THF are of comparable solvation power for polystyrene as are the other good solvents, benzene and toluene. Thus, for the interpenetration parameter $\psi = A_2M^2/4\pi^{3/2}N_AR_g^3$, we obtained ψ=0.32±.03 for PS/THF, and ψ=0.21±.02 for PS/ETBZ. However, since we determine differing values of $\rho(\cong 1.3)$ with R_g= 1356A for PS in THF in comparison with $\rho(\cong 1.5)$ and R_g=1608A for PS/ETBZ, we

TABLE 1 Static and dynamic characteristics of polystyrene ($M_w=8.42\times10^6$) in tetrahydrofuran and ethylbenzene.

$D_t \times 10^8$ cm^2/s	4.32	3.30
R_h(Å)	1086	1068
$K_d \times 10^{-2}$ cm^3/gm	10.71	6.15
ρ	1.25	1.51
R_g(Å)	1356	1608
$A_2 \times 10^3$ molcm^3/g^2	.183	.140
ψ	.379	.179
$[\eta]$ cm^3/gm	1116	1000
τ_1, μs	1364	2490
A_1	1.293	.844
η, cp	.465	.619

infer that there are inherent differences in the nature of the internal chain hydrodynamics and perhaps also in the conformational state of the PS chains in these chemically distinct good solvent systems[2,4].

Figure 1 shows the scattering angle dependence of the values $(\bar{\Gamma}_2 - \bar{\Gamma}_1)_{c=o}$ and $\bar{\Gamma}_1/(\sin^2\theta/2)$ for PS in THF. A corresponding plot was also obtained for PS in ETBZ though it is not shown here. The quantity $\Gamma_1/(\sin^2\theta/2)$ was approximately independent of angle for both systems, indicating that the translational diffusion coefficient had been successfully separated from the internal modes. Values of k_d were determined from the concentration dependence of $\Gamma_1/(\sin^2\theta/2)$ for both polymer-solvent systems. Values of the dynamic form factor, $(P_o/P)_{c\to o}$ were obtained by extrapolation to the limit of zero concentration as $[a_1/(a_1 + a_2)]_{c=o}$. The quantity $(P_o/P)_{c\to o}$ decreases with increasing values of $q^2R_g^2(=X)$, as shown in Figure 2. The $(\Gamma_2-\Gamma_1)$ values at finite angles were found to be approximately independent of concentration and $(\Gamma_2-\Gamma_1)_{c\to o}$ was obtained as an average over all concentrations. The longest intramolecular relaxation time, τ_1, was determined from the low angle data as

$$\lim_{\substack{c=o \\ qR_g = 1.0}} (\Gamma_2 - \Gamma_1), = 2/\tau_1 \qquad (18)$$

The results for τ_1 listed in Table 1 show that these values are very different for polystyrene in the two good solvent systems studied. The τ_1 values in ETBZ are approximately twice those observed in THF. Finally, Figure 2 indicates that the quantity $(P_o/P)_{c\to o}$ decreases with X much more rapidly for PS/THF than for PS/ETBZ.

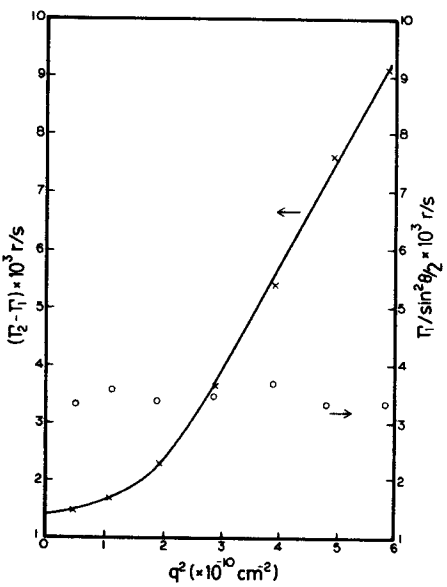

FIGURE 1

The translational diffusive decay rate $\bar{\Gamma}_1/q^2$ and the collective intramolecular relaxation rate $\bar{\Gamma}_2 - \bar{\Gamma}_1$ plotted against $q^2 \times 10^{-10}$ at infinite dilution for PS in THF.

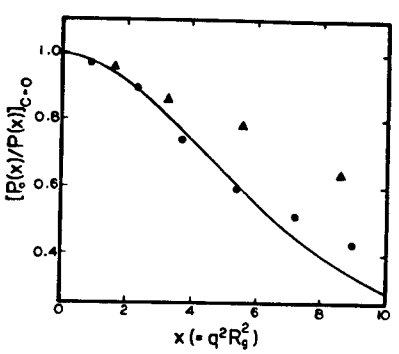

FIGURE 2

The relative scattered intensity of the translational mode $P_o(X)/P(X)$ at infinite dilution, as a function of $X(= q^2R_g^2)$ for PS in THF (●) and PS in ETBZ (▲). The solid line is a theoretical curve for an unperturbed flexible coil with dominant hydrodynamic interactions and preaveraged Oseen tensor[6,19].

DISCUSSION

The longest intramolecular relaxation time, τ_1, has been derived for gaussian chains from theories based on the bead-spring model

$$\tau_1 = M\eta_o[\eta]/A_1RT \qquad (19)$$

where M is the polymer molecular weight, η_o is the solvent viscosity, $[\eta]$ is the intrinsic viscosity, A_1 is a constant, R is the gas constant, and T is the absolute temperature. The parameter A_1 has been calculated in the two limiting cases, i.e. free and non-free draining. For the free draining Rouse[18] model, A_1=0.822 whereas for the non-draining Zimm[17] model, where the hydrodynamic interactions were preaveraged, the parameter A_1=1.184.

We can evaluate A_1 from eq. (19) by inserting our experimental values of η_1, $[\eta]$ and M_w. For PS/THF we have τ_1=1364 μs, $[\eta]$=1116 cm g^{-1}, and η_o= $4.65X10^{-3}$g cm^{-1} s^{-1} which yields A_1=1.29 ± 0.2, a result which is close to the Zimm prediction for non-draining chains. Likewise, for PS in ETBZ, with τ_1=2490 μs, η_o=$6.19X10^{-3}$g $cm^{-1}s^{-1}$ and $[\eta]$=1000 cm g^{-1}, eq. (18) yields A_1=0.84±0.1 which is quite different from the A_1 value obtained for PS in THF, and is closer to the Rouse prediction for free-draining chains. Of course any relationship between our results and these two theoretical values must be regarded as fortuitous since, a) the effect of preaveraging has not been evaluated, and b) the effect of excluded volume is not included[18,19].

Turning to our data for the variation of the dynamic form factor $(P_o/P)_{c\to o}$, we find a quite different dependence on the scaled scattering vector $X=q^2R_g^2$ for PS/THF versus PS/ETBZ as shown in Figure 2. In the range X<7 the results for PS/THF are in accord with a theoretical curve for non-draining gaussian chains[6,19]. On the other hand, the corresponding data for PS/ETBZ fall significantly above the theoretical prediction at X>2.0. Evidently, the scattering amplitude of the intramolecular motions for PS in ETBZ at a specified value of qR_g is smaller than in THF. It is interesting to note that the P_o/P values observed by us for PS in THF are comparable to those reported for flexible chains in theta solvents[6]. Conversely, the P_o/P values obtained for PS in ETBZ are similar to those observed by Nemoto et al.[7,8] in studies on the good solvent systems, polystyrene/benzene (BZ)[7] and polyisoprene (PIP)/cyclohexane (CH)[8]. It is also pertinent to note here that the systems PS/ETBZ, PS/BZ, and PIP/CH all have numerically comparable values of the ratio $\rho=R_{g,z}/R_h$ (≅1.5), different from the ρ values (≅ 1.3) obtained for PS in THF.[8] The values of ρ for PS in THF are similar to those reported for the theta solvent PS/trans-decalin[6], and the $(P_o/P)_{c\to o}$ values for PS/t-decalin exhibit comparable dependence on X to that shown in Figure 2 for PS in THF. Thus it seems that the quantity $(P_o/P)_{c\to o}$ appears, at least approximately, to exhibit universal scaling when plotted versus $X_h = q^2R_h^2$. This suggests that it is the hydrodynamic radius which determines the distribution of the total scattering amplitude between the internal and external modes.

The decrease in $(P_o/P)_{c=o}$ for PS in THF relative to PS in ETBZ can be interpreted qualitatively using the discussion of Perico et al.[19] for the non-draining gaussian chain model with preaveraged hydrodynamic interactions. These authors showed that as the strength of the hydrodynamic interaction increases, the contribution of the intramolecular motions to the total scattering amplitude is enhanced. Thus, Figure 2 supports the interpretation that the strength of the hydrodynamic interaction is higher for PS in THF.

In summary, our results for ρ_1, τ_1 and $(P_o/P)_{c=o}$ are consistent in that they indicate similar differences in the hydrodynamic properties of PS in

THF versus PS in ETBZ. Our observations may be interpreted as reflecting a greater degree of solvent draining in ETBZ, as indicated by a larger value of ρ_1, a smaller value of the hydrodynamic draining parameter, A_1[17], and a diminished contribution of the intramolecular modes to the dynamic light scattering spectrum[19]. To develop a more quantitative interpretation of our results, current theory for the hydrodynamic properties of flexible chains will need to consider such effects as excluded volume, internal friction and perhaps hydrodynamic screening.

ACKNOWLEDGMENT

We thank the Materials Research Laboratory for support of this work through research award NSF DMR86-14093.

REFERENCES AND NOTES

1) Mijnlieff, P.F., Wiegel, F.W. J. Polym.Sci.-Phys. Ed., 1980, 18, 1781.
2) McDonnell, M.E., Jamieson, A.M. J. Macro. Sci., Phys., 1977, B13, 67.
3) Miyaki, Y., Fujita, H. Macromolecules, 1981, 14, 742.
4) Venkataswamy, K., Jamieson, A.M. Macromolecules, 1986, 19, 124; Jamieson, A.M., Venkataswamy, K. Polym. Bull., 1984, 12, 275.
5) Douglas, J.F., Freed, K.F. Macromolecules, 1984, 17, 2354; Douglas, J.F., Freed, K.F. Macromolecules, 1984, 17, 2344.
6) Tsunashima, Y., Nemoto, N., Kurata, M. Macromolecules, 1983, 16, 1184; Tsunashima, Y., Hirata, M., Nemoto, N., Kurata, M. Macromolecules, 1983, 16, 584; Tsunashima, Y., Hirata, M., Nemoto, N., Kanjiwara, K., Kurata, M. Macromolecules, 1987, 20, 2862.
7) Nemoto, N., Makita, Y., Tsunashima, Y., Kurata, M. Macromolecules, 1984, 17, 425.
8) Tsunashima, Y., Hirata, M., Nemoto, N., Kurata, M. Macromolecules, 1987, 20, 1992.
9) Bhatt, M., Jamieson, A.M. Macromolecules, submitted.
10) Burchard, W., Schmidt, M., Stockmayer, W.H. Macromolecules, 1980, 13, 580.
11) Benmouna, M., Akcasu, A.Z. Macromolecules, 1978, 11, 1187.
12) Fixman, M. J. Chem. Phys., 1986, 84, 4085.
13) Benmouna, M., Akcasu, A.Z. Macromolecules, 1980, 13, 409.
14) Akcasu, A.Z., Han, C.C., Benmouna, M. Polymer, 1980, 21, 866.
15) Freed, K.F., Douglas, J.F., Wang, S.Q., Perico, A., "Polymer-Flow Interaction", 1985, AIP Conf. Proc. No. 137 (Amer. Inst. of Phys., NY).
16) Zimm, B.H. Macromolecules, 1980, 13, 592.
17) Zimm, B.H. J. Chem. Phys., 1948, 16, 1099.
18) Rouse, P.E. J. Chem. Phys., 1953, 21, 1272.
19) Perico, A., Piaggio, P., Cuniberti, C. J. Chem. Phys., 1975, 62, 2690.
20) Berry, G.C. J. Chem. Phys., 1966, 44(12), 4550.
21) Koppel, D.E. J. Chem. Phys., 1972, 57, 4818.
22) Pecora, R. J. Chem. Phys., 1968, 49, 1032.
23) Stock, R.S., Ray, W.H. J. Polym. Sci.: Polym. Phys. Ed., 1985, 23, 1393.
24) Marquardt, D.S., SIAM, J. Appl. Math., 1963, 11, 431.
25) Yamakawa, H., "Modern Theory of Polymer Solutions", 1971, Harper and Row, NY; Kirkwood, J.G. Riseman, J. J. Chem. Phys., 1948, 16, 565.
26) Ostrowsky, N., Sornette, D., Parker, P., Pike, E.R. Opt. Acta, 1981, 28, 1059.
27) McWhirter, J.G., Pike, E.R. J. Phys. A.: Math Nucl. Gen., 1978, 11, 1729.
28) McWhirter, J.G. Opt. Acta, 1980, 27, 83.
29) Spychaz, T., Lath, D., Berek, D. Polymer, 1979, 20, 437.

Accepted April 25, 1988 C